SANDIA REPORT

SAND2002-0086
Unlimited Release
Printed March 2002

Microdiagnostic Lab on a Chip

Maarten P. de Boer, Norman F. Smith, Michael B. Sinclair, Michael S. Baker, Fernando Bitsie

Prepared by
Sandia National Laboratories
Albuquerque, New Mexico 87185 and Livermore, California 94550

Sandia is a multiprogram laboratory operated by Sandia Corporation, a Lockheed Martin Company, for the United States Department of Energy under Contract DE-AC04-94AL85000.

Issued by Sandia National Laboratories, operated for the United States Department of Energy by Sandia Corporation.

Available to DOE and DOE contractors from
U.S. Department of Energy
Office of Scientific and Technical Information
P.O. Box 62
Oak Ridge, TN 37831

Telephone: (865)576-8401
Facsimile: (865)576-5728
E-Mail: reports@adonis.osti.gov
Online ordering: http://www.doe.gov/bridge

Available to the public from
U.S. Department of Commerce
National Technical Information Service
5285 Port Royal Rd
Springfield, VA 22161

Telephone: (800)553-6847
Facsimile: (703)605-6900
E-Mail: orders@ntis.fedworld.gov
Online order: http://www.ntis.gov/ordering.htm

SAND 2002-0086
Unlimited Release
Printed March, 2002

Microdiagnostic Lab on a Chip
LDRD Final Report

Maarten P. de Boer
MEMS and Novel Si Technology Dept.

Norman F. Smith
Radiation & Reliability Physics Dept.

Michael B. Sinclair
Information Discovery Extraction & Analysis Dept.

Michael S. Baker
MEMS Device Technologies Dept.

Fernando Bitsie
Electromechanical Engineering Dept.

Sandia National Laboratories
P. O. Box 5800
Albuquerque, NM 87185-1080

Abstract

Polycrystalline silicon (polysilicon) surface micromachining is a new technology for building micrometer (μm) scale mechanical devices on silicon wafers using techniques and process tools borrowed from the manufacture of integrated circuits. Sandia National Laboratories has invested a significant effort in demonstrating the viability of polysilicon surface micromachining and has developed the Sandia Ultraplanar Micromachining Technology (SUMMiT V^{TM}) process, which consists of five structural levels of polysilicon. A major advantage of polysilicon surface micromachining over other micromachining methods is that thousands to millions of thin film mechanical devices can be built on multiple wafers in a single fabrication lot and will operate without post-processing assembly. However, if thin film mechanical or surface properties do not lie within certain tightly set bounds, micromachined

devices will fail and yield will be low. This results in high fabrication costs to attain a certain number of working devices. An important factor in determining the yield of devices in this parallel-processing method is the uniformity of these properties across a wafer and from wafer to wafer. No metrology tool exists that can routinely and accurately quantify such properties. Such a tool would enable micromachining process engineers to understand trends and thereby improve yield of micromachined devices.

In this LDRD project, we demonstrated the feasability of and made significant progress towards automatically mapping mechanical and surface properties of thin films across a wafer. The MEMS parametrics measurement team has implemented a subset of this platform, and approximately 30 wafer lots have been characterized. While more remains to be done to achieve routine characterization of all these properties, we have demonstrated the essential technologies. These include:

(1) well-understood test structures fabricated side-by-side with MEMS devices,
(2) well-developed analysis methods,
(3) new metrologies (i.e., long working distance interferometry) and
(4) a hardware/software platform that integrates (1), (2) and (3).

In this report, we summarize the major focus areas of our LDRD project. We describe the contents of several articles that provide the details of our approach. We also describe hardware and software innovations we made to realize a fully automatic wafer prober system for MEMS mechanical and surface property characterization across wafers and from wafer-lot to wafer-lot.

Acknowledgements

We would like to acknowledge the staff in the microelectronics development lab at Sandia National Laboratories for fabrication of the test structures used in this LDRD project. We also thank the MEMS parametric team, including Scott Swanson, Fredd Rodriguez, Andy Oliver, Danelle Tanner and Sita Mani, who used hardware and software tools developed in this LDRD work to generate Fig. 5 in this report. Sandia is a multiprogram laboratory operated by Sandia Corporation, a Lockheed Martin Company, for the United States Department of Energy under Contract DE-AC04-94AL85000.

Table of Contents

Figures

Microdiagnostic Lab on a Chip LDRD Final Report

Introduction

Freestanding thin films are created by surface micromachining. Useful microdevices such as accelerometers, gyroscopes, image correctors, printheads, flow sensors, drug delivery modules and computers performing mechanical logic, to name a few, can be fabricated. Because the substrate has been removed from the thin film, it is also theoretically possible to attain extraordinary resolution on thin film mechanical properties and to obtain new information on surface properties such as adhesion and friction. Also, because these films are deposited by thin film technology methods with inherent cross-wafer nonuniformities, device yield can be affected by mechanical and surface property variations. The goal of this LDRD project was to develop test structures, metrologies, analysis tools and an integrated platform to measure mechanical and surface properties across a wafer, so that fabrication yield of these devices can be improved. Thin film mechanical properties of interest include film curvature κ (due to stress gradient through the thickness of a film), Young's modulus E (i.e., stiffness), residual stress σ_R, and fracture strength σ_F. Thin film surface properties include adhesion, adhesion hysteresis, friction and wear. In most cases, a given test structures is sensitive to the property of interest as well as to test structure non-idealities. These non-idealities must be identified, quantified and accounted for in the test structure model in order to accurately extract the property of interest.

Test Structure Criteria

Although test structures have been previously developed to measure these various properties, there existed no framework for measuring all of them on a single instrument. For routine measurement of such properties, it is essential that such an instrument be available. Therefore, in this LDRD project, we focused heavily on developing an integrated set of test structures, metrologies and analysis methods such that all these properties could be measured using only one instrument. We believe that it is necessary to meet certain criteria if a given test structure is to continually be used in the future. The complete list of test structure criteria deemed essential were as follows:

Test structures developed for *process monitoring* must ...

1) be fabricated according to a standard (e.g., SUMMiT V^{TM}) process flow and be tested on-chip without special handling.
2) require only a small area on the chip so that the majority of the real estate can be devoted to the MEMS device.
3) use electrostatics to provide force, as this is the means of actuation in MEMS.
4) allow deflections to be measured at the nanometer scale so that the property of interest can be known to high confidence and can be used to predict deflections at loading conditions other than those used to determine the property.
5) be non-destructively tested so that properties measured can later be validated independently, and so that no particles are generated.
6) all be tested on the same instrument.
7) be testable at the wafer level so that testing can be accomplished before packaging.
8) be tested and analyzed rapidly.

Focus Area #1 - Integrated Approach

In Fig. 1, we show schematically how many of the criteria just listed can be satisfied. In Fig. 1(a) (top center of Fig. 1), a MEMS chip (repeated approximately 60 times over a six inch wafer) is shown. Areas designated by ovals indicate the area occupied by the test structures we developed. The MEMS chip in Fig. 1(a) is surrounded by representations of test structures (Figs. 1(b)-(f)) that fit inside the small oval areas. These test structures are designed to be sensitive to a property of interest. They are electrostatically actuated, their deflections are measured by interferometry and test structure models then analyze the deflections to determine the property. By measuring at multiple electrostatic loadings, multiple measurements are inferred without damaging the device. Therefore, the measurements are verifiable and the test structures are reusable. Interferometry enables measurements at the nanometer scale, allowing the test structure area and the number of test structures used to be small. The implementation of these concepts satisfies criteria #1-#6 in the list above. For the basic mechanical properties (elastic and residual stress), these test structures now are in place in all five structural levels on SUMMiT V^{TM} wafer lots. For the less commonly measured properties (adhesion, friction and fracture strength), the structures are in place in one or two structural levels.

The first major focus of our LDRD was then to develop these test structure and the analysis concepts. We showed that the use of interferometry to measure point-by-point deflections to determine properties of MEMS compares favorably with other test structure analyses [5]. Our methods for analyzing deflections of electrostatically loaded cantilevers as in

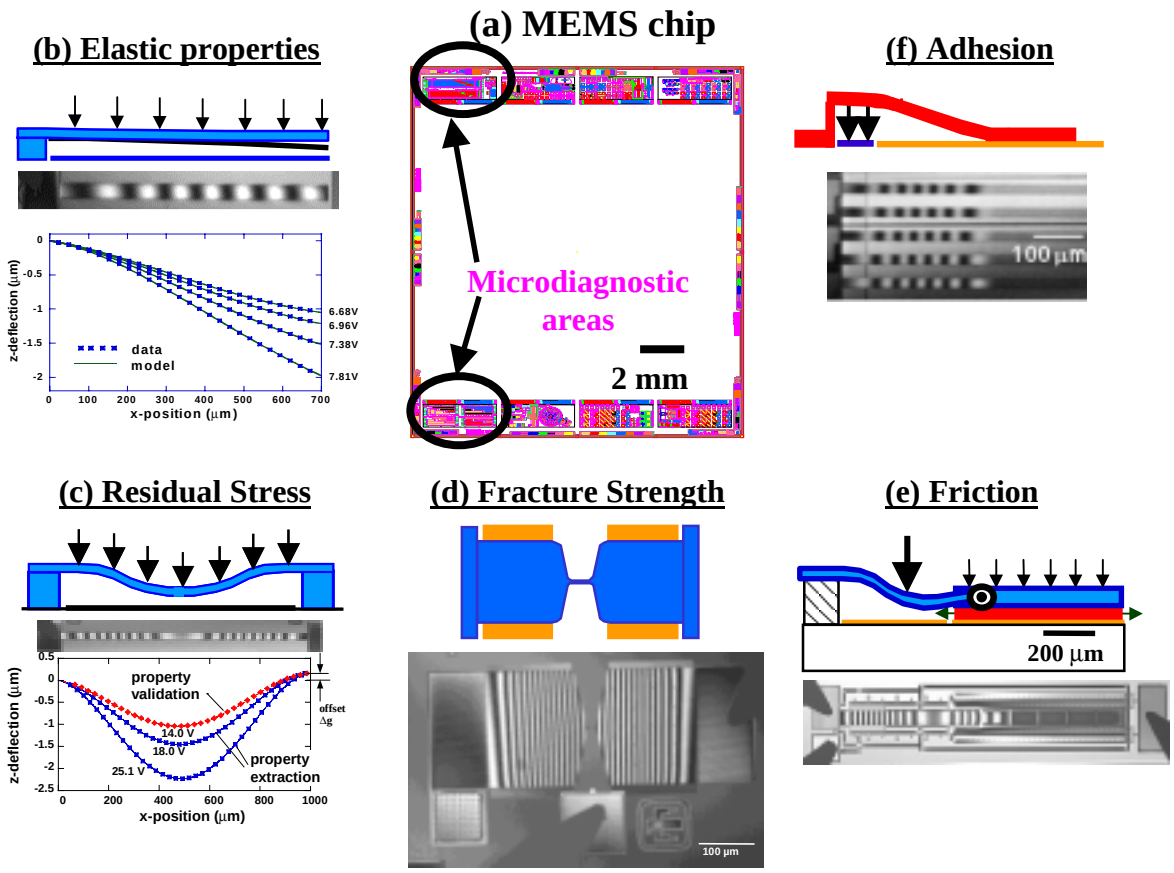

Fig. 1 Test structures, interferograms and analysis results for the microdiagnostic lab on a chip LDRD project. (a) These structures fit into only a small area of a MEMS chip as denoted by the ovals, allowing parametric analysis of multiple polysilicon layers across a wafer and from run to run. (b) cantilevers for elastic properties, (c) fixed-fixed beams for residual stress, (d) tapered fixed-fixed beam for strength measurement, (e) cantilevers with actuation pad near support post for adhesion measurement, and (f) hinged friction pad for friction measurement.

Fig. 1(b) to accurately determine thickness t, gap g, takeoff angle θ_o, curvature κ, Young's modulus E and support post compliance β are detailed in [6]. Also, a significant advantage of interferometry over purely electrical probing techniques (e.g., capacitance or "pull-in" measurements) that stems from obtaining the full deflection curve is that the 95% confidence levels for a given property can be determined for each measurement [6]. Our methods for accurately determining residual stress σ_R as in Fig. 1(c) are reported in [7]. In particular, we have devised a method that takes advantage of the deflection data to determine boundary conditions. This allows us to determine σ_R without resorting to the finite element method to model the support posts, greatly reducing analysis time. Our test structure and technique for determining fracture strength σ_F as in Fig. 1(d) is described in [10]. This device amplifies force

first by converting work done out-of-plane at large displacement to work done in-plan at small displacment. A second level of force amplification is achieved by a large width reduction in the fixed-fixed beam. Sandia submitted the idea for the fracture device to the patent office [1]. Improved friction test structures as in Fig. 1(e) have been described in [14] and [18]. These structures enable measurement of friction over a wide pressure-velocity space. An advanced method for measuring adhesion of a beam to a substrate as in Fig. 1(f) is reported in [8]. With this method, we are able to measure adhesion and adhesion hysteresis (i.e., stiction) along the entire length of a cantilever beam. The publications associated with these structures are posted on our website at

http://www.sandia.gov/mems/micromachine/biblog_char.html or

http://www.sandia.gov/mems/micromachine/biblog_summit.html.

We have worked closely with the American Society for Testing and Materials (ASTM) to begin to establish standards for measuring properties in MEMS. The National Institute of Standards and Technology (NIST) has written preliminary standards using a minor variant on our methods. Also, we published two articles [5, 9] in an ASTM Special Technical Publication (STP) to help influence the setting of these standards.

Focus Area #2 - Long Working Distance Interferometry

The second major focus of the LDRD was to develop hardware for an instrument to allow testing at the wafer level, in the interest of satisfying criterion #7 in the list on p. 5. Although interferometry gives us deflection information at the nanometer scale as required to achieve the accuracy and confidence levels we need, commercially available interferometers are not compatible with testing at the wafer level. This is because the free working distance between the interferometry attachment and the wafer surface is 5 mm or less. Electrical probes that are routinely used to apply voltages to devices on MEMS wafers are 10-15 mm high, and hence do not fit under an interferometer attachment. Therefore, we developed a long working distance interferometer, as seen in Fig. 2, which allows standard probes or a probe card to be used while obtaining interferograms. The interferometer was fabricated to be compatible with the zoom optics of the original probe station microscope, and therefore could be directly mounted on the

original probe station. Fig. 2(a) shows the interferometer mounted on the probe station, Fig. 2(b) demonstrate the one-inch (25 mm) free working distance, while Fig. 2(c) shows the high quality interferograms obtained. Sandia submitted a patent application based on this interferometer design, which was laser-based [2]. Later, an improved interferometer was also designed based on incoherent illumination. A technical advance has been submitted for this later innovation as well [3]. The advantages of this later advance include (i) speckle-free images, (ii) capability for determining thickness information across discontinuous surfaces and (iii) easy stroboscopic imaging. We intend to submit an article for journal publication on these new interferometers. Also, other Sandia staff have expressed interest in these designs. For example, Richard Shagum (Firing Set & Optical Eng. Dept. 2612) has replicated our design [3] and is using it for testing MEMS under cryogenic conditions. Furthermore, the long working distance interferometer is extremely useful for characterization of MEMS devices [18].

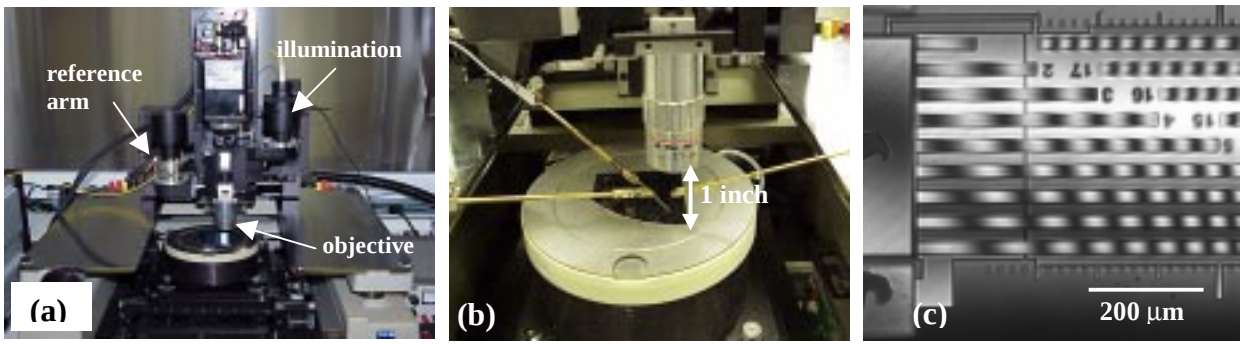

Fig. 2 (a) Modified microscope on probe station, (b) closeup of objective with 2.5 cm free working distance, (c) interferogram of cantilever beam array.

Focus Area #3 - Automation and Wafer Mapping

The third focus of the LDRD was to automate the data taking and analysis procedures in the interest of satisfying criterion # 8 in the list on p. 5. We made significant progress in this area [9], and Sandia submitted a patent application [4]. We call the integrated approach "Interferometry for Materials Property Determination in MEMS" (IMaP). Three software routines were developed to enable rapid property determination, as portrayed in Fig. 3. Interferograms of unloaded beams are taken using an image analyzer program called "LineProfile Tool". Within this program, reference points indicating the beginning and end of the beam, as well as reference points indicating where the linescan begins and ends (i.e., 1st pixel

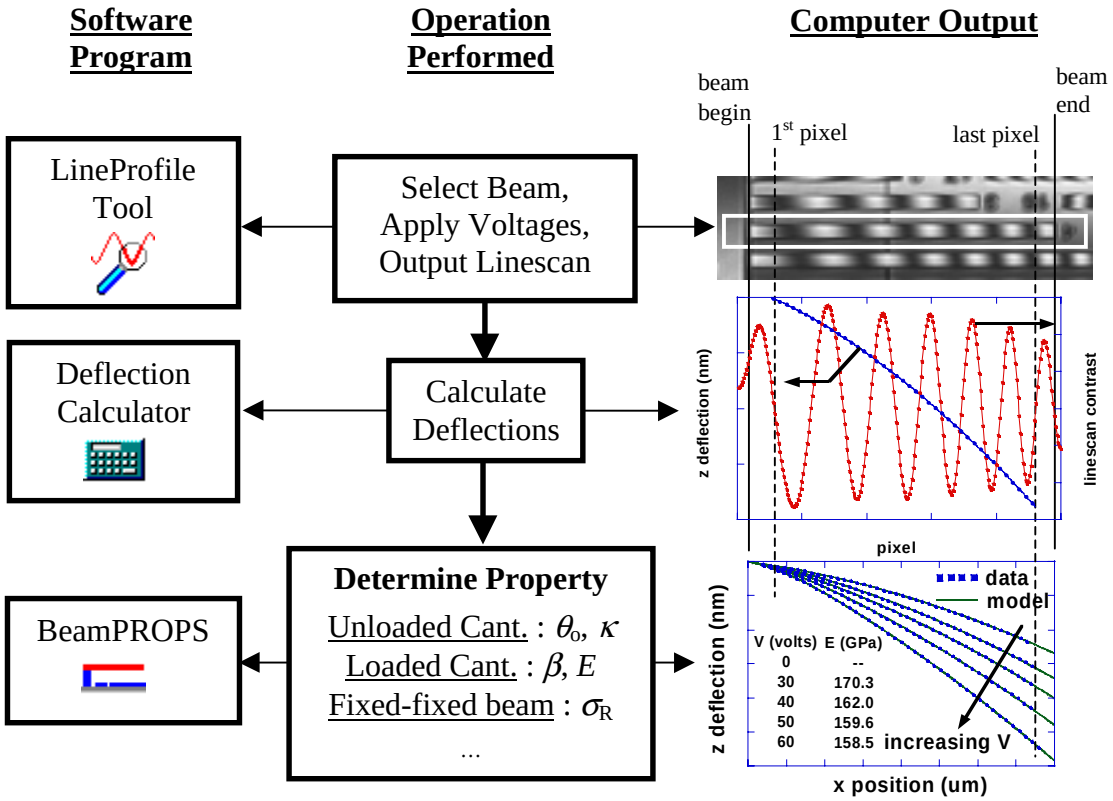

Fig. 3 Overview of algorithms to determine properties of MEMS test structures within the IMaP framework.

and last pixel), are superposed on the image. The linescan, containing fringe information as a function of pixel position, along with the reference information and the beam length, are stored in a file for further processing by a program called "Deflection Calculator". It converts the linescan information into pixel by pixel *z*-deflection data with near nm resolution, and also converts pixel data into *x*-position data. A program called "BeamPROPS" operates on the deflection data to extract properties. BeamPROPS calculates model deflections by the finite difference method. For unloaded beams, it accounts for the non-idealities takeoff angle θ_o and beam curvature κ; and for the small effect of gravity. It determines the properties by adjusting the model deflections until the error between the data and the model deflections are minimized using a quasi-Newton search algorithm.

Figure 4 shows testing results of mechanical properties along a column of chip sites as represented in Fig. 4(a), for the third level of polysilicon, "Poly 3". Fig. 4(b) shows tight control of thickness, with t=2.34 +/- 0.02 μm. Gap height g was measured interferometrically to ~20 nm

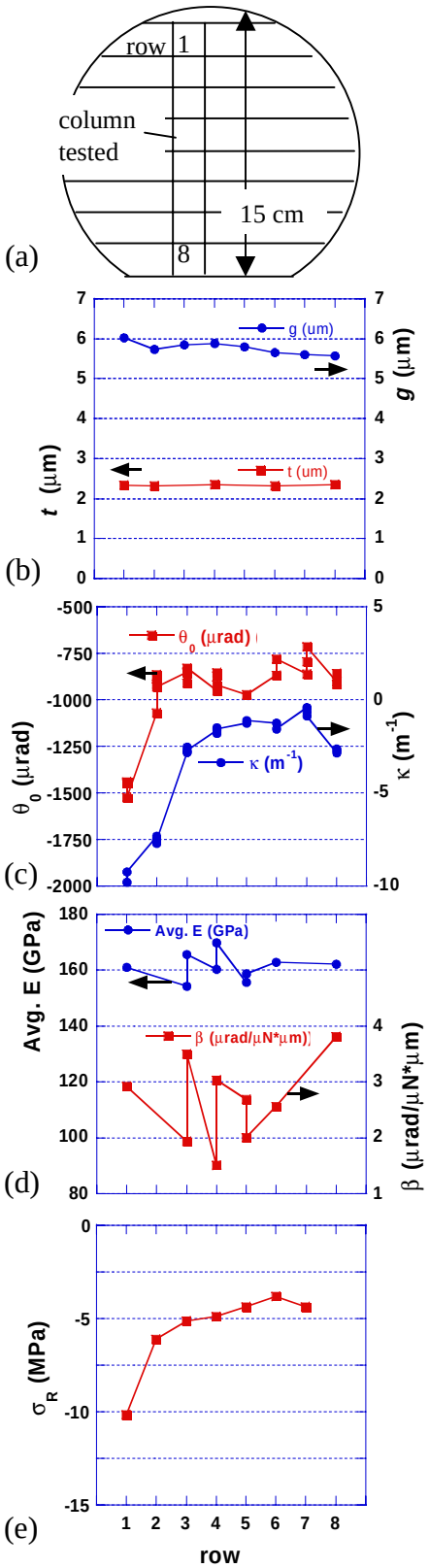

Fig. 4 Column map for materials properties (a) wafer, (b) t, g, (c) θ_o, κ, (d) E, β, (e) σ_R

accuracy on cantilevers actuated into contact with the substrate. Poly 3 gap height g is not as well controlled as thickness, with values from 5.53 to 6.03 μm. This variation along the wafer column can be explained by the nonuniformities in the chemical mechanical polishing (CMP) that is applied to planarize the oxide layer underlying Poly 3. It is important to measure the geometrical properties t and g at this accuracy level (~20 nm) on each individual device, because the subsequent analysis to determine E depends strongly on these values.

Optimum values of unloaded cantilever takeoff angle θ_o and κ are shown in Fig. 4(c). It is seen that θ_o is negative but relatively constant across the wafer, with values of –750 to –1000 μradians. The negative values of θ_o result from oxide incorporation within the support post structure. After release, the highly compressive oxide is no longer constrained, and induces the support to pivot. This is undesirable because it forces long cantilevers to touch the substrate, reducing the effectiveness of the test structures, but has been improved with a better support post layout. Values of κ from -1 to -2.5 m^{-1} (corresponding to stress gradient values of –0.16 to -0.4 MPa/μm) are quite low for MEMS devices. Note in row 1 that θ_o drops sharply to –1500 μrad and also that κ decreases significantly to –10 m^{-1}. The change in κ may be due to a subtle microstructural feature or trace contaminant such as the oxygen level being different in the Poly 3 layer at this die location relative

to the rest of the wafer. This in turn may be responsible for the sharp drop in θ_o. Clearly, both negative θ_o and negative κ are undesirable for MEMS devices that often contain long structural elements assumed to be flat over the substrate.

In Fig. 4(d), the values of *E* are seen to be relatively constant across the substrate. This is expected because it is unlikely that the subtle changes in stress gradient at the sub MPa/μm level (or the changes in σ_R at <10 MPa, see below) will affect the bulk modulus of ~163 GPa expected for our isotropically textured films. However, it is important to note that given the highly non-linear mechanics of the electrostatically actuated beam, this result can only be achieved because *t*, *g*, θ_o and κ were measured and modeled on the same individual cantilevers. The average value of β~2.5 μrad/(μN*μm) compares well with finite element modeling of similar geometries, where β values of 2.47 to 2.73 μrad/(μN*μm) were determined [6]. However, we see in Fig. 4(d) that β varies significantly across the wafer without a trend. Because its value is dominated by the polysilicon thickness which was well controlled, we would not expect that β would vary to this degree. We investigated this issue and found that errors of 100% in β result if there is a 2 pixel error (~ 5 μm) in the starting location of the beam ("*x*-offset error"). This is a book-keeping issue because the location of the beginning of the beam is effectively being reassigned. Fortunately, a 2 pixel *x*-offset error induces a change in *E* of less than 4% [6].

The values of residual stress σ_R, while typically low in magnitude at ~ -5 MPa, correlate well with curvature κ, as seen by comparing Fig. 4(c) to Fig. 4(e). This has been observed by other authors and is not a necessary outcome of the processing but is perhaps not surprising because κ is caused by the gradient in σ_R through the thickness of the film. The high stress resolution inherently available from the interferometry enables correlation at the subtle levels of change in stress observed here (compare Fig. 4(c) to 4(e)). The correlation between κ and σ_R along the wafer column suggests that control of stress gradient and residual stress may be affected by the same processing non-uniformities.

Lot-to-Lot Variation

A subset of our methodology is being used to characterize MEMS parametrics on wafer lots. Figure 5 shows the dependence of curvature before and after a change in the process. A value of κ=0 is desired, and it can be observed that this is more closely achieved after the process change was made.

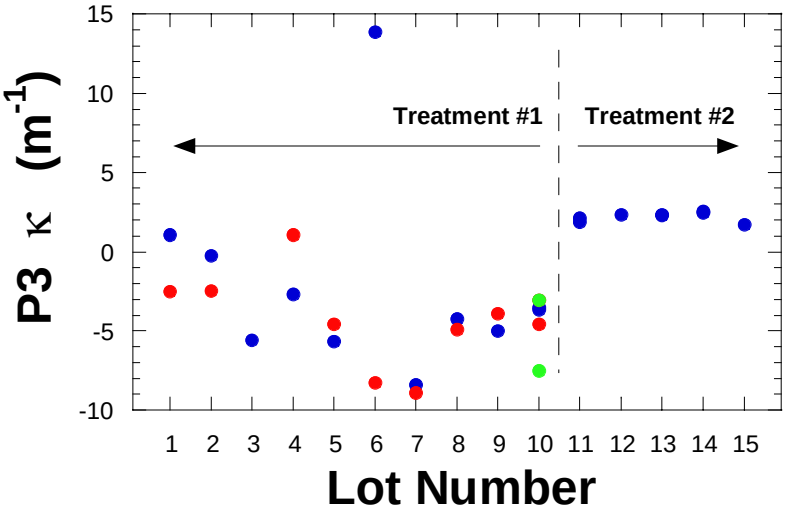

Fig. 5 Curvature of SUMMiT V™ Poly 3 layer versus lot number.

Interest in Licensing IMaP

U.S. companies have shown significant interest in licensing portions of IMaP. One company (Coventor) has already 3 licensed IMaP patents. We are working with Paul M. Smith of the Licensing & IP Management Dept. 1321 to determine the best course to take in building a commercial IMaP instrument.

Student Contributions

Master's degree level students from several universities contributed to the success of this project. They helped develop analysis tools, designed and laid out test structures, and also assisted in experiments. Publications of these students in association with the project are listed below. One student (Michael S. Baker) was hired as a staff member at Sandia. The students, their universities and their advisers include:

Student	University	Adviser
Brian Jensen	Brigham Young University	Professor Larry Howell
Brian Crozier	Washington State University	Professor David Bahr
Nathan Masters	Brigham Young University	Professor Larry Howell
Michael Baker	Brigham Young University	Professor Larry Howell
Emily Pryputniewicz	Worcestor Polytechnic Institute	Prof. Ryszard Pryputniewicz
Kamili Jackson	Johns Hopkins University	Prof. William Sharpe
David Luck	Univ. of Colorado at Boulder	Prof. Y.C. Lee

Patents and Publications

Patents

[1] M. P. de Boer, F. Bitsie and B. D. Jensen, "*Electrostatic Apparatus for Measurement of Microfracture Strength"*, SD6596/S93881 **(submitted to U.S. patent office)** (2000).
[2] M. B. Sinclair, N. F. Smith and M. P. de Boer, "*Long Working Distance Interference Microscope"*, SD-6697/S-95517 **(submitted to U.S. patent office)** (2000).
[3] M. B. Sinclair and M. P. de Boer, "*Long Working Distance Incoherent Light Interference Microscope"*, **(technical advance submitted to SANDIA patent office)** (2001).
[4] M. P. de Boer, B. D. Jensen, S. L. Miller, N. F. Smith and M. B. Sinclair, "*Method and System for automated on-chip material and structural certification of MEMS devices"*, SD-6497/S-93739 **(submitted to U.S. patent office)** (1999).

Journal Papers

[5] N. D. Masters, M. P. de Boer, B. D. Jensen, M. S. Baker and D. Koester, *Side-by-side comparison of passive MEMS strain test structures under residual compression*, in Mechanical properties of structural thin films, Special Technical Publication (STP) No. 1413; **accepted**, edited by S. B. Brown and C. L. Muhlstein (ASTM, West Conshohocken, PA, 2002).
[6] B. D. Jensen, M. P. de Boer, N. D. Masters, F. Bitsie and D. A. LaVan, *Interferometry of actuated cantilevers to determine material properties and test structure non-idealities in MEMS*, J. MEMS **10** (3), 336 (2001).
[7] M. S. Baker, M. P. de Boer, N. F. Smith and M. B. Sinclair, *Determination of residual stress in fixed-fixed Microbeams to ± 0.5 Megapascal accuracy* , J. MEMS **submitted** (2001).
[8] J. A. Knapp and M. P. de Boer, *Mechanics of microcantilever beams subject to combined electrostatic and adhesive forces*, J. MEMS **submitted** (2001).
[9] M. P. de Boer, N. F. Smith, N. D. Masters, M. B. Sinclair and E. J. Pryputniewicz, *Integrated platform for testing MEMS mechanical properties at the wafer scale by the*

IMaP methodology, in Mechanical properties of structural thin films, Special Technical Publication (STP) No. 1413; **accepted**, edited by S. B. Brown and C. L. Muhlstein (ASTM, West Conshohocken, PA, 2002).

Conference Papers

[10] M. P. de Boer, B. D. Jensen and F. Bitsie, *A small area in-situ MEMS test structure to measure fracture strength by electrostatic probing*, Proceedings of the SPIE, vol. 3875, Santa Clara, CA, (1999), pp. 97-103.

[11] B. D. Jensen, M. P. de Boer and S. L. Miller, *IMaP: Interferometry for materials property evaluation in MEMS*, MSM '99, San Juan, Puerto Rico, (1999), pp. 206-209.

[12] B. D. Jensen, M. P. de Boer and F. Bitsie, *Interferometric measurement for improved understanding of boundary effects in micromachined beams*, Proceedings of the SPIE, vol. 3875, Santa Clara, CA, (1999), pp. 61-72.

[13] M. S. Baker, M. P. de Boer, N. F. Smith and M. B. Sinclair, *Measurement of residual stress in MEMS to sub megapascal accuracy*, Society for Experimental Mechanics Annual Conference and Exposition, Portland, OR, (2001),

[14] B. T. Crozier, M. P. de Boer, J. M. Redmond, D. F. Bahr and T. A. Michalske, *Friction measurement in MEMS using a new test structure*, Mater. Res. Soc. Proc., vol. 605, Boston, MA, (2000), pp. 129-134.

Other papers supported in part by this LDRD funding

[15] M. P. de Boer, J. A. Knapp, T. A. Michalske, U. Srinivasan and R. Maboudian, *Adhesion hysteresis of silane coated microcantilevers*, Acta Mater. **48** (18-19), 4531 (2000).

[16] M. P. de Boer and T. M. Mayer, *Tribology of MEMS*, MRS Bull. **26** (4), 302 (2001).

[17] M. P. de Boer, J. A. Knapp and P. J. Clews, *Effect of nanotexturing on interfacial adhesion in MEMS*, International Conference on Fracture, **accepted**, Honolulu, HI, (2001).

[18] M. P. de Boer, D. L. Luck, J. A. Walraven and J. M. Redmond, *Characterization of an inchworm actuator fabricated by polysilicon surface micromachining*, Proceedings of the SPIE, vol. 4558, San Francisco, (2001), pp. 169-180.

[19] G. C. Brown, R. J. Pryputniewicz, M. P. de Boer and N. F. Smith, *Dynamics of MEMS microengines using optoelectronic laser interferometry*, Mater. Res. Soc. Proc. **605** , (2000) pp. 163-168.

[20] B. C. Bunker, R. W. Carpick, R. Assink, M. L. Thomas, M. G. Hankins, J. A. Voigt, D. L. Sipola, M. P. de Boer and G. L. Gulley, *The impact of solution agglomeration on the deposition of self-assembled monolayers*, Langmuir **16** , 7742 (2000).

[21] J. P. Sullivan, T. A. Friedmann, M. P. de Boer, D. A. LaVan, R. J. Hohlfelder, C. I. H. Ashby, M. T. Dugger, M. Mitchell, R. G. Dunn and A. J. Magerkurth, *Developing a new material for MEMS: Amorphous Diamond*, Mater. Res. Soc. Proc. **657**, (2001), pp. E7.1.1-E7.1.9.

[22] J. J. Sniegowski and M. P. de Boer, *IC-compatible polysilicon surface micromachining*, Annu. Rev. Mater. Sci. **30** , 297 (2000).

Distribution

1	MS	9018	Central Tech. Files, 8945-1
2		0899	Technical Library, 9616
1		0612	Rev. & Appr. Desk, 9612 for DOE/OSTI
1		0188	Donna Chavez, 1030
1		1081	Fred Sexton, 1762
1		1081	Danelle Tanner, 1762
1		1080	Jay Jakubczak, 1703
1		1080	Harold Stewart, 1749
1		1080	Michael Shaw, 1749
1		1080	Sita Mani, 1749
1		1080	Tom Lemp, 1749
1		1411	Michael Sinclair, 1812
1		0886	Nancy Jackson, 1812
1		0329	Fernando Bitsie, 2614
1		0329	Gerald Sleefe, 2614
1		0329	Mark Polosky, 2614
1		0329	Frank Peter, 2614
1		0329	Andy Oliver, 2614
1		1080	David Sandison, 1769
1		1080	Michael Baker, 1769
1		1080	Jeff Dohner, 1769
1		1380	Paul M. Smith, 1321
1		1077	Tom Zipperian, 1740
1		0961	Carol Adkins, 14101
5		1080	Maarten de Boer, 1749

This page intentionally left blank